Diffusive Relaxation Mode in Poly(styrene-*b*-methylphenylsiloxane) Copolymer Melts above and below the Order–Disorder Transition

S. Vogt,† T. Jian,‡ S. H. Anastasiadis,‡ G. Fytas,*,‡ and E. W. Fischer†

Foundation for Research and Technology—Hellas, Institute of Electronic Structure and Laser, P.O. Box 1527, 711 10 Heraklion, Crete, Greece, and Max-Planck-Institut für Polymerforschung, P.O. Box 3148, 6500 Mainz, Germany

Received December 14, 1992; Revised Manuscript Received February 15, 1993

ABSTRACT: Photon correlation spectroscopy in the polarized mode has been used to investigate the dynamics of the composition fluctuations in three poly(styrene-*b*-methylphenylsiloxane) bulk copolymers. A new diffusive relaxation process has been measured at different temperatures in the disordered (samples S1 and S2) and ordered (S3) state. We interpret the diffusion in S1 and S2 as originating from the relaxation of the equilibrium composition configurations ("pattern") and the diffusion in S3 as arising from the motion of polystyrene microdomains (cylinders) dispersed in the mobile poly(methylphenylsiloxane) microphase. The vastly different temperature dependence of the pattern and the microdomain diffusion coefficients resemble the temperature dependence of the copolymer zero shear viscosity and the bulk poly(methylphenylsiloxane) viscosity, respectively.

I. Introduction

Diblock copolymers consist of a contiguous linear sequence of polymerized monomers of chemical species A (i.e., the A block) covalently bonded to a second contiguous linear sequence of monomers of a different chemical species B. Since the entropic and enthalpic contributions to the free energy density scale as N^{-1} and χ, respectively, it is the product χN that dictates the equilibrium phase morphology for a certain composition f, where N is the total number of segments and χ is the A–B segment–segment Flory–Huggins interaction parameter.[1] For $\chi N \ll 1$, the equilibrium morphology is a melt with uniform composition (homogeneous or disordered state). As χN increases to be $O(10)$, a delicate balance between entropic and enthalpic factors leads to an order–disorder transition (ODT) toward a microphase characterized by long range order in its composition with a characteristic size of the order of the size of the molecules.[2-4] At $\chi N \gg O(10)$, the domination of enthalpic terms leads to highly organized periodic domain microstructures.[5]

In a seminal work, Leibler[2] constructed a Landau expansion of the free energy to fourth order in a compositional order parameter field, $\psi(\boldsymbol{r}) = \phi_A(\boldsymbol{r}) - f$, where $\phi_A(\boldsymbol{r})$ is the microscopic volume fraction of A monomers at position $\boldsymbol{r}$, and he was able to map out the phase diagram of a diblock copolymer near the ODT. Fredrickson and co-workers[3,4] extended Bravoskii's[6] self-consistent Hartree approximation method in order to incorporate fluctuation corrections in the effective Hamiltonian for a diblock melt. The fluctuation corrections, controlled by a Ginsburg parameter, $\bar{N}$, defined[7] by $\bar{N} = 6^3(R_G^3\rho_c)^2$, where ρ_c is the number density of copolymer chains in the melt and R_G is the copolymer radius of gyration, lead to a suppression of the symmetric critical mean field point that is replaced by a weak first order transition at a lower temperature. Moreover, the amplitude of the ordered composition profile is predicted to be $O(\bar{N}^{-1/6})$ at the ODT. Besides the extremum composition field configurations weighted by Leibler's mean field theory, namely the uniform field in the disordered phase and the perfectly ordered sinusoidal configuration of wavelength $2\pi/q^* \cong O(R_G)$ in the ordered phase, the Hartree approximation also weights configurations that have superimposed isotropic composition plane waves with wave vectors having random orientations and phases and a preferred[3] or not[4] magnitude, q^*. The theory suggests that the root-mean-squared amplitude of these fluctuations is $O(\bar{N}^{-1/6})$, comparable to the amplitude of the long range ordered composition field. The typical equilibrium field configurations ("pattern") in the disordered diblock melt (which fluctuate in time) were speculated[7] to be reminiscent of the transient nonequilibrium patterns encountered during the intermediate and late stages of spinodal decomposition,[8] based on a symmetric Cahn construction of the structure factor.[9]

A recent polarized photon correlation spectroscopic (PCS) study of a disordered diblock copolymer melt has revealed the presence of a new diffusive relaxation process.[10] This mode was attributed to the relaxation of the equilibrium composition field configurations ("pattern") present in the "homogeneous state", above the microphase separation temperature (MST) or ODT. This transient pattern picture is in accord with the observation of two vastly different segmental relaxation rates in rheologically and calorimetrically homogeneous diblock copolymer melts.[11] However, no theory exists for the dynamics of the composition field configurations, albeit it is believed that crossing into the ordered state will lead to a more permanent pattern, coherent over large distances. On the other hand, no significant change in the amplitude of the composition profile is predicted near the ODT.[3]

In this study we investigate the diffusional dynamics of three poly(styrene-*b*-methylphenylsiloxane) copolymers above and below the ODT in the bulk using PCS in the polarized geometry. The main objective is to exploit structural effects on the dynamics of composition fluctuations at low wave vectors (q) extending the first preliminary PCS study.[10] The diffusion of the block copolymer molecules in the bulk is very little explored. So far, there are two real time experiments on the self-diffusion of block copolymers. These concern copolymer chain diffusion in the couple partially deuterated/hydrogenated symmetric poly(ethylenepropylene-*b*-ethylethylene)[12] and in a dye-labeled symmetric poly(styrene-*b*-1,4-isoprene) film[13] mixed with identical unlabeled chains

* To whom correspondence should be addressed.
† Max-Planck-Institut für Polymerforschung.
‡ Institute of Electronic Structure and Laser.

0024-9297/93/2226-3357$04.00/0

using respectively forward recoil spectrometry and forced Rayleigh scattering. The forward recoil measurements, however, were hindered by the fact that annealing of diblock copolymer thin films produces an ordered morphology[14] with microdomains oriented parallel to the surface, that deters the diffusion.

II. Theoretical Background

The intensity of the polarized light scattering by the concentration fluctuations ("pattern") is related to the structure factor, $S(q)$, and the scattering amplitude by

$$I_c(q) = (a_1 - a_2)^2 S(q) \tag{1}$$

where a_i is the scattering length of the ith environment. In the Hartree approximation,[3] the structure factor $S(q)$ for a monodisperse diblock is modified from Leibler's mean field result to be

$$N/S(q) = F(x,f) - 2\chi_{eff}N \tag{2}$$

where

$$F(x) = \frac{g_1(1,x)}{g_1(f,x)g_1(1-f,x) - 1/4[g_1(1,x) - g_1(f,x) - g_1(1-f,x)]^2} \tag{3}$$

related to certain Debye correlation functions of a Gaussian block copolymer

$$g_1(f,x) = 2[fx + e^{-fx} - 1]/x^2 \tag{4}$$

with $x = q^2R_G^2$, $R_G^2 = Nb^2/6$, and b the statistical segment length. The effective interaction parameter, χ_{eff}, depends on temperature, molecular weight, and composition and is related to the bare parameter by

$$\chi_{eff}N = \chi N - \frac{C(f)}{2N^{1/2}}[F(x^*,f) - 2\chi_{eff}N]^{-1/2} \tag{5}$$

where $C(f)$ and $F(x^*,f)$ are composition-dependent coefficients[3] and $x^* = (q^*)^2R_G^2$, with q^* being the position of the maximum in $S(q)$. The Hartree structure factor near the ODT may be approximated by the Lorentzian form

$$S(q) = S_0/[1 + \xi^2(q - q^*)^2] \tag{6}$$

where the susceptibility $S_0 = (\epsilon\rho_c)^{-1}$ and the coherence length of composition fluctuations $\xi = \sqrt{6}cR_G\epsilon^{-1/2}$, with $\epsilon = F(x^*,f) - 2\chi_{eff}N$ and c a composition-dependent constant.[3] Theory predicts a finite correlation length for finite $\bar{N}$ at the ODT, $\xi_c = 5.4663cR_G[C(f)]^{-1/3}(\bar{N})^{1/6}$.

For a real copolymer, the function $F(x,f)$ should be modified to account for polydispersity effects that strongly influence the low-q scattering behavior. Assuming that polydispersity arises mainly through the polymerization kinetics and can be modeled with a Shultz–Zimm distribution, Burger et al.[15] found that the Debye functions $g_1(f,x)$ should be modified as

$$\overline{g_1}(\bar{f},\bar{x}) = 2[\bar{f}\bar{x} + \langle\exp(-f_K x)\rangle_n - 1]/\bar{x}^2 \tag{7}$$

$$\overline{g_1}(1,\bar{x}) = 2[\bar{x} + \langle\exp(-x)\rangle_n - 1]/\bar{x}^2 \tag{8}$$

where $\bar{x} = \langle N\rangle_n b^2q^2/6$, $\langle\exp(-f_K x)\rangle_n = \{1 + U_K\bar{f}_K\bar{x}\}^{-1/U_K}$, and $\langle\exp(-x)\rangle_n = \langle\exp(-f_A x)\rangle_n\langle\exp(-f_B x)\rangle_n$. $\langle N\rangle_n$ is the number average number of segments, $U_K = (M_w/M_n)_K - 1$ of block K related to the total polydispersity by $U_{total} = U_A f^2 + U_B(1-f)^2$. Usually, it is assumed that $U_A = U_B$. Inclusion of polydispersity corrections leads to a shift in the position of the maximum at q^* to lower q's and a significant increase in the structure factor at the low light scattering q's.

Table I. Molecular Characteristics of the Samples

sample	w_{PS}	φ_{PS}	$10^{-3}M_n$	M_w/M_n	T_g (K)	q^* (Å^{-1})	T_{ODT} (K)
S1	0.47	0.49	10.5	1.12	303	0.049	
S2	0.23	0.24	30.5	1.06	247, 340[a]	0.034	
S3	0.21	0.22	59.0	1.05	247, 364	0.026	403

[a] Weak broad glass transition.

The prediction of large amplitude composition fluctuations near the ODT has significance but only for the thermodynamic–static properties but also for the dynamic–transport properties of block copolymers. Indeed, rheological measurements on several diblock copolymers[7,16] have shown evidence of substantial fluctuation enhancement of the shear viscosity and first normal stress coefficients in the pretransitional disordered state. A theory to describe such enhancements has been developed[17,18] which qualitatively captures the relative fluctuation contributions to the shear and normal stress coefficients but fails to predict the magnitude by 1 order of magnitude.[16] The essential physics embodied in the theory is that as $\chi N \to (\chi N)_{ODT}$, the mean fluctuation amplitude increases, thereby presenting additional resistance to the long range motion of polymer chains. In order for a molecule to move a distance greater than $O(R_G)$, it must overcome the potential barrier created by the local excesses of each block associated by the fluctuating pattern. Dissipation of these local composition fluctuations (i.e., pattern relaxation) requires the cooperative movement of many molecules within a correlation volume of characteristic size ξ and, accordingly, should occur at frequencies well below the longest single chain relaxation time. The shortcoming of the theory is attributed to the expression used for the Onsager coefficient that describes the concentration flux generated by an imposed chemical potential gradient. The biased reptation estimate[19] used did not incorporate the effects of a strongly inhomogeneous environment on the dynamics of individual copolymers.

In the previous work,[10] the effective self-diffusion constant of the fluctuating pattern was modeled using the Stokes–Einstein formula

$$D = k_BT/(6\pi\eta\xi) \tag{9}$$

for the diffusion of moieties of size[3] ξ in an environment with zero shear viscosity η and an average local friction coefficient dominated by the slow component (k_B is Boltzmann's constant, and T is the temperature), in analogy to the blob model of the cooperative diffusion constant in concentrated polymer solutions,[20] that has been shown to be applicable to the self-diffusion in pure liquids with surprising good results.[21]

III. Experimental Section

Sample Characteristics. The poly(styrene-*b*-methylphenylsiloxane), P(S-*b*-MPS), diblock copolymer samples were synthesized by anionic ring-opening polymerization of 1,3,5-trimethyl-1,3,5-triphenylcyclotrisiloxane and characterized as described elsewhere.[22] The molecular characteristics of the three samples are listed in Table I. Sample S1 displays a homogeneous morphology with one single but broad glass transition (T_g), whereas sample S3 was found to be rheologically and calorimetrically heterogeneous. For sample S2, the ODT appears to fall below T_g(PS) and hence becomes less obvious.[23] The complex modulus, $G^*(\omega) = G'(\omega) + jG''(\omega)$, $j^2 = -1$, was measured on a Rheometrics RMS-800 mechanical spectrometer, using 50-mm-diameter parallel plate geometry, in the frequency range 0.1–100 rad/s and for temperatures −20 to +180 °C. The rheological response for the homogeneous samples is similar to that of a "simple" viscoelastic liquid, where time–temperature superposition holds and $G''(\omega) \sim \omega^1$ at low ω's. For the heterogeneous sample S3, the superposition principle fails at low ω and low temperature and shows an $\omega^{1/2}$ dependent at low ω's. Good optical

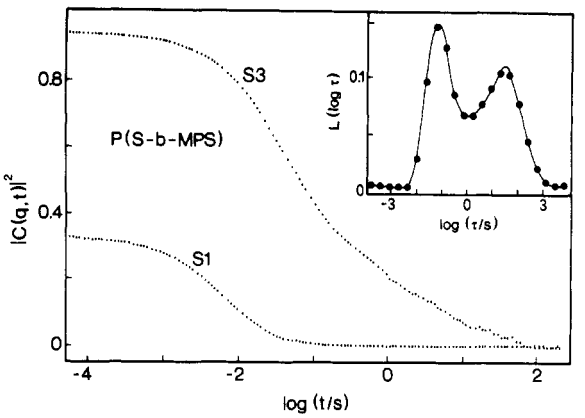

Figure 1. Composition correlation functions $|C(q,t)|^2$ for the "disordered" (S1) and "ordered" (S3) sample at 150 °C and $q = 2.78 \times 10^{-3}$ Å^{-1}. The distribution $L(\log \tau)$ (eq 11) of correlation times for S3 is shown in the inset.

quality samples suitable for homodyne PCS experiments were obtained by direct filtration from the melt through a 0.45-μm millipore filter into the light scattering cell (12.7-mm o.d.) under pressure at about 140 °C. The appropriateness of the prepared specimens for PCS measurements is evident by the light scattering power of the samples, over the whole temperature range of the experiments. The polarized light scattering intensity varies for S1–S3 from 3 to 10 times the polarized light scattering intensity of pure toluene, as will be discussed in section IV.

Photon Correlation Spectroscopy (PCS). The correlation function $G(q,t)$ of the polarized (VV) light scattering intensity at different scattering angles θ was measured with an ALV-5000 full digital correlator covering a wide time range (10^{-6}–10^{3} s). The light source was an Ar^+ laser (Spectra Physics 2020) with wavelength $\lambda = 488$ nm operating at a 150-mW single mode. Both the incident beam and scattered light were polarized perpendicular (VV) to the scattering plane. For homodyne conditions, the measured $G(q,t)$ at a given scattering vector $q = (4\pi n/\lambda)\sin(\theta/2)$ (n being the refractive index of the medium and θ the scattering angle) is related to the desired normalized field correlation function $C(q,t)$ by

$$G(q,t) = A[1 + f^*|\alpha C(q,t)|^2] \tag{10}$$

where A is the baseline, f^* is an instrumental factor, and α is the fraction of the total polarized scattered intensity arising from, in principle, density, composition, and orientation fluctuations with correlation times longer than about 10^{-6} s. The PCS measurements were performed at different temperatures over the range 70–200 °C. The samples were first annealed at 150 °C, i.e., above the highest T_g and the ODT of S3, and then slowly cooled to the measurement temperature. Especially for S3 below the ODT (~130 °C) annealing the sample for 24 h did not have any measurable effect on the experimental correlation functions.

IV. Results

Figure 1 shows two experimental net correlation functions ($(G(q,t)/A - 1)/f^* \equiv |C(q,t)|^2$) for samples S1 and S3 at $\theta = 90°$ ($q = 2.78 \times 10^{-3}$ Å^{-1}) and 150 °C. Over the temperature (T) range of the measurements, the dynamics of the density and orientation fluctuations associated with the primary relaxation processes[11] near T_g are much faster and, moreover, are characterized by a q-independent broad distribution of relaxation times. Therefore, the narrow relaxation functions of Figure 1 are dominated by composition fluctuations associated with the pattern relaxation. The slow process observed for sample S3 is attributed to slow density fluctuations ("clusters") usually found in molecular and macromolecular glass formers[24] at low T near T_g. Nevertheless, the relaxational characteristics of the desired fast mode can reliably be extracted from the experimental $C(q,t)$, unless significant overlapping is present.

In the absence of the slow mode (at high T), the experimental correlation functions can be described by a single exponential decay. However, to consider the contribution of the slow process, we have chosen for consistent fitting the inverse Laplace transform (ILT) of $C(q,t)$:

$$C(q,t) = \int_{-\infty}^{\infty} L(\ln \tau) \exp(-t/\tau)\, \mathrm{d} \ln \tau \tag{11}$$

The distribution relaxation function $L(\ln \tau)$ is shown as an inset in Figure 1. The average relaxation time obtained from $L(\ln \tau)$ was found to depend on the magnitude of q. Figure 2 shows the diffusive ($\propto q^2$) character of the experimental fast relaxation rate of S3 for two temperatures and allows the determination of the diffusion coefficient $D = 1/(\tau q^2)$. The values of the latter for the three samples are listed in Table II and shown in Figure 3 as a function of temperature, to be discussed in section V later.

An estimate of the light scattering intensity (I_c) associated with this diffusive process can be obtained from the relative amplitude, a, deduced from the ILT of $C(q,t)$, and the total polarized light scattering intensity I. If we neglect contributions from orientation and density fluctuations, $I_c = aI$. The corresponding static structure factor is

$$S(q) = R(q)\lambda^4\rho/(2\pi n(\mathrm{d}n/\mathrm{d}\varphi)^2) \tag{12}$$

where $R(q) = (I_c/I_T)(n/n_T)^2 R_T$ with R_T, I_T, and n_T being respectively the Rayleigh factor of the standard (toluene), its polarized scattering intensity, and the refractive index and ρ being the number density. For the increment $\mathrm{d}n/\mathrm{d}\varphi$ we have used the difference between the refractive

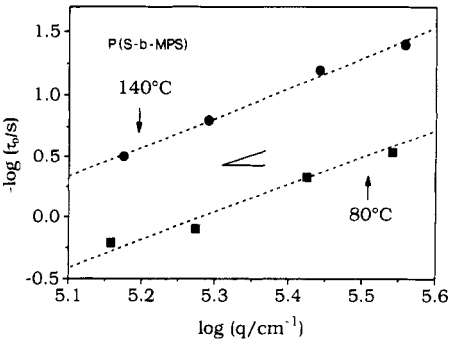

Figure 2. Dependence of the fast relaxation rate for S3 on the magnitude of the scattering vector q at two temperatures. The dashed lines represent least squares fits to the experimental points. The slope of 2 for diffusive behavior is indicated in the plot.

Table II. Diffusion Coefficient in P(S-b-MPS) Bulk Copolymers[a]

	D (cm^2/s)		
T (K)	S1	S2	S3
473.2	8.4×10^{-9}		
448.2	2.4×10^{-9}		
423.7	5.9×10^{-10}	3.8×10^{-10}	9.2×10^{-10}
418.4	5.4×10^{-10}		
413.2	4.4×10^{-10}		1.4×10^{-10}
408.2	3.3×10^{-10}		
403.2	1.8×10^{-10}	1.8×10^{-10}	1.2×10^{-10}
398.4	1.6×10^{-10}		
393.7		4.8×10^{-11}	1.1×10^{-10}
387.6	6.0×10^{-11}		
383.2	3.0×10^{-11}	7.9×10^{-11}	6.6×10^{-11}
377.4		4.4×10^{-12}	
373.2	1.3×10^{-11}	1.2×10^{-12}	
370.4		6.7×10^{-13}	
363.6			4.2×10^{-11}
353.4			3.2×10^{-11}
342.5			1.8×10^{-11}

[a] Experimental uncertainty is about 10%.

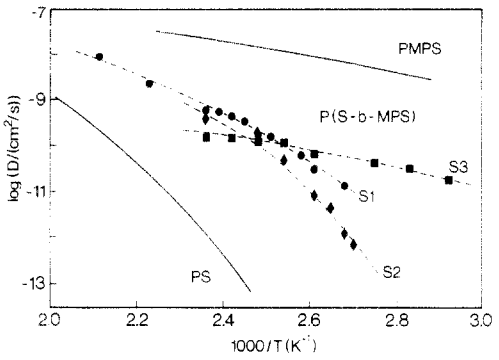

Figure 3. Arrhenius plot of the diffusion coefficients D for the three P(S-*b*-MPS) diblock copolymers. The experimental uncertainty is given by the size of the symbols, and the dashed lines denote the WLF fits. The two solid lines denote the self-diffusion coefficients, D_s, for the two bulk homopolymers (M_n = 21 000).

Table III. Parameters of the Fluctuation Theory at 140 °C

sample	N_{PS}*[a]	N*[b]	$\bar{N}$	χ	χ_{eff}	ϵ	ξ (Å)	ξ_c (Å)
S1	48	99	540	0.030	0.020	17	20	83
S2	65	266	1453	0.030	0.019	26	31	103
S3	114	509	2780	0.030				

[a] $N_{PS}^* = N_{PS}v_{PS}/v_{ref}$; $v_{ref} = (v_{PS}v_{PMPS})^{1/2}$. [b] $N^* = N_{PS}^* + N_{PMPS}v_{PMPS}/v_{ref}$.

indices of PS and PMPS homopolymers. Owing to the presence of both fast and slow ("cluster" scattering) density fluctuations, the fraction of the total intensity is less than 1. The ratio I_c/I_T is virtually T independent and amounts to 1 and 3, respectively, for the "disordered" and "ordered" samples S1 and S3. At 140 °C and for $q = 2.78 \times 10^{-3}$ Å^{-1}, the measured structure factors are 3, 14, and 11 for samples S1, S2, and S3, respectively. For the disordered samples S1 and S2, the magnitude of $S(q)$ correlates with the proximity to the ODT, whereas sample S3 is below the ODT and light scattering probably arises from supramolecular (domain) structures, as is discussed below.

V. Discussion

"Pattern" Relaxation. The fluctuation of the instantaneous composition configurations spatially with time can cause dynamic light scattering intensity at low q's ($\sim 2.8 \times 10^{-3}$ Å^{-1}). For the present system, both the amplitude $(a_1 - a_2)$ and $S(q)$ in eq 1 are finite. The former is related to the volume fractions in the two microenvironments, which are probed by depolarized PCS[10,11,25] and for sample S1 are[10] 0.77 and 0.33 in PS (compared to the average 0.49). The calculated structure factor[3,15] for 140 °C and $q = 2.78 \times 10^{-3}$ Å^{-1}, estimated from eqs 2–8, amounts to 3.4 and 1.9 for samples S1 and S2. The calculated $S(q)$ compares with the experimental values, taking into account the experimental uncertainties in $S(q)$ and in the χ values[26] used in the computation (the parameters for the fluctuation theory calculations are shown in Table III). Moreover, the parameter $\bar{N}$ is relatively low for the theory[3] to quantitatively assess the fluctuation effects. Nevertheless, the prediction of equilibrium composition fluctuatons near and above the ODT is in accordance with the present diffusive process in P(S-*b*-MPS) diblock copolymers. The polarized light scattering intensity was found to be virtually independent of the scattering vector q, as expected for scatterers with size ξ such that $q\xi \ll 1$.

The dynamics of these composition fluctuations are characterized by the diffusion coefficient D which is probably controlled by chain diffusion in the "inhomogeneous" environment with characteristic size ξ of the order of $R_G(\bar{N})^{1/6}$. The variation of D with temperature is shown in the Arrhenius plot of Figure 3. The increased contribution of the slow ("cluster") process in the experimental correlation functions of S2 and S3 above 150 °C has precluded measurements at even higher temperatures. The diffusion coefficients for samples S1 and S2 exhibit very similar T dependence, which is much stronger than that of S3. Furthermore, the T variation of D for S1 and S2 resembles that of the self-diffusion D_s of bulk homopolymer PS,[13,27] whereas for S3 it mimics that of the D_s of bulk PMPS. The latter was determined for a homopolymer with M_n = 20 000 at 25 °C by pulsed-field gradient nuclear magnetic resonance and extended to other T's using the Williams–Landel–Ferry[28] (WLF) equation of PMPS with T_g = 248 K and WLF coefficients C_{1g} = 10.5 and C_{2g} = 56 K estimated[29] from the T dependence of the shear viscosity. For comparison, the WLF parameters for PS with T_g = 373 K are C_{1g} = 13.7 and C_{2g} = 57 K.

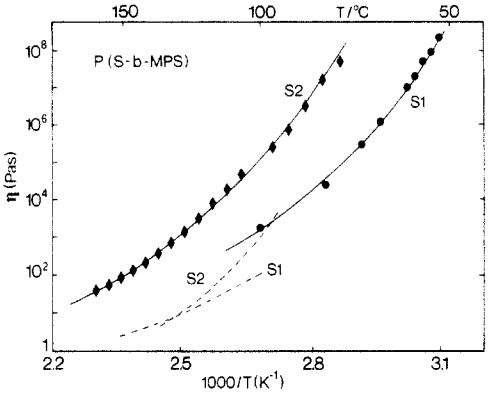

Figure 4. Arrhenius plot of the shear viscosity $\eta = \lim_{\omega \to 0} G''(\omega)/\omega$ for the two disordered P(S-*b*-MPS) diblock copolymers (S1, S2).[26] The solid lines represence WLF temperature fits. The dashed lines denote the temperature dependence of the computed η (eq 9) using the experimental D and ξ of Table III.

The experimental finding that D for samples S1 and S2 (which are above the ODT) and D_s of PS display similar T dependences mandates that the "pattern" relaxation is dominated by the higher friction coefficient ζ of PS-rich microregions, in agreement with the preliminary results.[10] The frictions ζ_{PS} and ζ_{PMPS} of the two homopolymers are vastly different in the T range of the experiment. The much faster D compared to D_s of PS is mainly due to the lower T_g of the PS microregions in S1 and S2. In fact, the experimental D values for S1 and S2 can be represented by the same WLF coefficients C_{1g} and C_{2g} of bulk PS with effective T_g about 313 and 333 K, respectively, for S1 and S2. The trend in the estimated T_g values is expected in view of the higher PS composition φ_{PS} in the hard microregions of S2 relatively to S1, which is supported by the local segmental dynamics within PS- and PMPS-rich microenvironments.[10,25] Therefore, the pattern relaxation is dominated by the lower diffusivities of the PS block.

An attempt to quantitatively account for the values of D in S1 and S2 is based on eq 9. In this expression, the value of the correlation length ξ (Table III) depends sensitively on the χ parameter. At the ODT, however, the upper limit[3] ξ_c is independent of χ and equal to 83 and 103 Å, respectively, for S1 and S2. The computed η (eq 9) using the values of ξ from Table III can be compared with the experimental macroscopic zero shear viscosity[26] calculated as $\eta = \lim_{\omega \to 0} G''(\omega)/\omega$, shown in Figure 4, where $G''(\omega)$ is the dynamic shear loss modulus at frequency ω. As expected from the comparison between D and D_s of PS, the temperature dependence of the computed and experimental η is quite similar; the viscosity of the diblock copolymer is dominated by the stiffer (PS) component. The computed η is, however, lower than the viscosity of S1 and S2 by a factor of 15 and 80, respectively. This

disparity becomes even larger if ξ_c were used in eq 9. Apart from the uncertainties in the ξ values, it becomes obvious that pattern relaxation requires a lower η than shear deformation, and the local ordering has a greater effect on shear modulus than on diffusion. In fact, the latter shows a discontinuity at the ODT[7,16] whereas there is no noticeable effect on D_s by approaching the ODT.[12,13,30] Lower viscosity values may correspond to frequencies higher than the frequency $(1/\tau_1)$ characterizing the longest relaxation time of the diblock, i.e., the frequency at which $G''(\omega)$ and $G'(\omega)$ cross.[31] However, in the present case the diffusion times are much longer and, therefore, the low frequency limit viscosity may be compared to our estimations (Figure 4).

The q^2-dependent diffusive "pattern" relaxation mode discussed herein should not be confused with the internal relaxation mode predicted by mean field theory.[32,33] In the absence of composition fluctuations, the random phase approximation[32] and the Edwards Hamiltonian approach[33] predict a single relaxation process for homogeneous diblock copolymer melts, that is attributed to the internal relative motion of the two blocks. The relaxation rate of this process, however, is predicted to be independent of the scattering vector, q, for the low q's of light scattering. The internal mode has been experimentally observed earlier in diblock copolymer solutions[34] and very recently for homogeneous diblocks in the bulk[35] together with the q^2-dependent "pattern" diffusion for a series of poly(dimethylsiloxane-b-methylethylsiloxane) diblocks of much higher molecular weights than the ones in the present system (N between 530 and 1110). The data for the internal mode agree with theory for both the q and N dependence of the relaxation rate and amplitude.[35]

"Domain" Relaxation. The diffusive process in S3 exhibits a distinctly different behavior than in S1 and S2. The former displays a weak T dependence compared to the other two samples (Figure 3), and the variation of D with T is rather similar to that of D_s of PMPS. In accordance with this finding, the relaxation rate $1/\tau_D(q)$ $(=Dq^2)$ should depend on the segmental time τ_S(PMPS) within PMPS-rich microregions rather than on τ_S(PS) within microenvironments rich in PS. In fact, the local τ_S(PS), measured by PCS in the depolarized geometry[36] is comparable with $\tau_D(q)$ which is referred to a much longer scale ($1/q \cong 350$ Å). Moreover, there is no signature of the T_g of the PS microenvironment on $\tau_D(q)$ in contrast to the segmental times, τ_S(PS), shown in Figure 5c. Above and below the T_g of the PS-rich microphase the mechanism of the diffusive process is the same, supported also by the intensity data of Figure 5b. The relative intensity $I^* = I_c/I_T$, where I_c is associated with the diffusive relaxation mode, is insensitive to the temperature variation over the examined T range. The relative I^* in Figure 5b is about 3 times higher than that for the disordered S1. These consistent findings imply that the diffusive mode in S3 cannot be assigned to the pattern relaxation discussed in the preceding section.

Sample S3 is both calorimetrically and rheologically ordered below 130 °C. The higher of the two glass transition temperatures of 364 K (Table I) is close to the T_g of PS (T_g = 371 K) and the temperature at which τ_S(PS) of Figure 5c exhibits the characteristic kink. The dynamic shear loss modulus $G''(\omega)$ changes from the terminal ω into an $\omega^{1/2}$ frequency scaling region as the system transfers to the ordered state.[7,16] Thus the ratio $G''(\omega)/\omega$ of Figure 5a, which is the shear viscosity for the disordered S1 and S2 in Figure 4, increases with different rates as T decreases below about 130 °C. The variation of $G''(\omega)/\omega$ with T is clearly different than that of Figure 4.

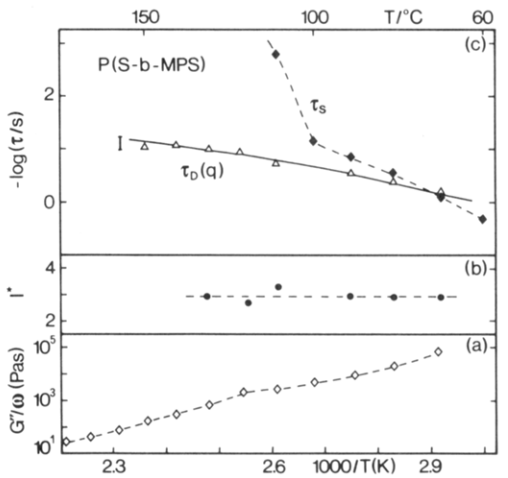

Figure 5. (a) Ratio $\lim_{\omega\to 0} G''(\omega)/\omega$ for S3[26] as a function of T. The different behavior compared to the viscosity data of Figure 4 is an indication of the ordered structure of S3 below about 130 °C. (b) Ratio $I^* = I_c/I_T$ of the intensity I_c associated with the fast diffusive mode in the ordered S3, to the polarized light scattering intensity I_T of toluene at different temperatures. (c) Arrhenius plot of the diffusive relaxation time $\tau_D(q) = 1/(D{\cdot}q^2)$ at $q = 2.78 \times 10^{-3}$ Å^{-1} and the q-independent segmental relaxation time τ_s within PS-rich microphases.[36] The solid line represents the fit of the WLF temperature equation to τ_D.

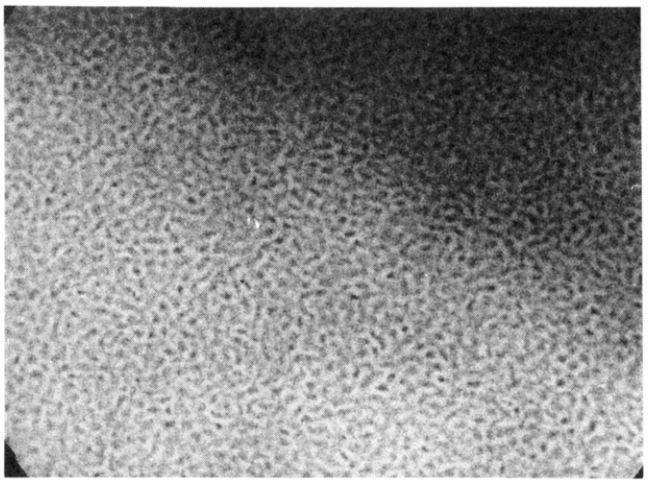

Figure 6. Inelastic transmission electron darkfield micrograph[37] at an energy loss of 270 eV. Scale bar corresponds to 0.1 μm.

In the ordered state, S3 with $\varphi_{PS} = 0.22$ should display[1] a hexagonal arrangement of cylinders with PS subchains in the hard core dispersed in the mobile PMPS (lower T_g) phase. The inelastic transmission electron darkfield micrograph[37] of Figure 6 recorded on a TEM-Zeiss 902 at 80 kV confirms the ordered morphology, with the black spots[37] being the PS microphase. The long period from small-angle X-ray scattering at 25 °C is measured to be d = 310 Å. For a cylindrical morphology, the radius of the cylinders is related to the volume fraction of PS by $R_{PS} = (\varphi_{PS} d^2/\pi \sin 60)^{1/2} = 88$ Å, close to the estimated value from the micrograph, that is larger than the unperturbed end-to-end distance of the PS subchains (73 Å), due to chain extension in the order state.[5]

To account for the value of D in S3, we picture the diffusive mode as the translational diffusion of the microstructured cylinders in the mobile PMPS matrix (white areas in Figure 6). The former defines the radius of the diffusing moiety whereas the latter determines the drag force. Equation 9, can now be used to compute the effective viscosity η^* from the experimental D for diffusing moieties of radius R_{PS}. At 80 °C, $D = 2.0 \times 10^{-11}$ cm^2/s and hence $\eta^* = 17$ Pa·s. Due to the somewhat increased

friction caused by the presence of PS in the PMPS environment, this value should be larger but of the same order of magnitude with the viscosity of bulk PMPS (N = 395). In fact, the macroscopic viscosity of the latter, estimated from the viscosities of two PMPS samples[29] with N = 240 and 5000, amounts to 7 Pa·s at 80 °C, whereas the macroscopic viscosity of S3 at 80 °C is about 2×10^4 Pa·s. The mobile PMPS microphase, therefore, allows for relatively fast microdomain diffusion in S3 comparable to the diffusion of S1 and S2. In contrast, a strong drop (by about 5 orders of magnitude) in the diffusion coefficient has been reported at the ordering transition of micelles of an ABA triblock copolymer in a highly selective solvent, probed by forced Rayleigh scattering.[38] Above about 20 wt % ABA, the formation of a regular 3-dimensional macrolattice of spherical micelles leads to this dramatic decrease in the diffusion coefficient of the micelles. In our case, however, the development of the 2-dimensional hexagonal macrolattice is accompanied by a significant decrease in the friction coefficient of the matrix microphase that counterbalances the ordering effect on the diffusion. The coherence of the macrolattice should, in principle, influence the "domain" diffusion. However, annealing sample S3 below the ODT for 24 h did not show any measurable slow down of the diffusion, implying that coarsening of the ordered morphology is a very slow process in these highly viscous bulk systems. In this context it should be noted that in microstructured diblock copolymer solutions the increase of the coherence of grains influences significantly both the dynamics and the static light scattering intensity.[39]

The change of the mechanism for the diffusive mode in disordered (S1, S2) and ordered (S3) P(S-*b*-MPS) diblock copolymers could be further elucidated by extending the PCS measurements well above the ODT of S3. Unfortunately, this was not feasible because of the very weak T dependence of χ[26] and the presence of significant "cluster" scattering even above 150 °C. However, we are currently investigating this diffusive process in a poly(styrene-*b*-1,4-isoprene)/toluene system, for which the ODT can readily be reached via variation of either T and/or copolymer concentration.

In summary, photon correlation spectroscopy in the polarized geometry has been used to investigate the diffusive relaxational dynamics of diblock copolymers both above and below the order–disorder transition temperature. Above the ODT, the relaxation process is identified as the relaxation of the composition field configurations induced "pattern", that is controlled by the friction coefficient of the slow microenvironment. Below the ODT and for cylindrical morphology, the relaxation mode is the diffusion of the dispersed microphase in the environment of the matrix and is controlled by the friction coefficient of the dispersing microphase.

References and Notes

(1) Bates, F. S.; Fredrickson, G. H. *Annu. Rev. Phys. Chem.* **1990**, *41*, 525.
(2) Leibler, L. *Macromolecules* **1980**, *13*, 1602.
(3) Fredrickson, G. H.; Helfand, E. *J. Chem. Phys.* **1987**, *87*, 697.
(4) (a) Barrat, G. L.; Fredrickson, G. H. *J. Chem. Phys.* **1991**, *95*, 1282. (b) Olvera de la Cruz, M. *Phys. Rev. Lett.* **1991**, *67*, 85.
(5) Helfand, E.; Wasserman, Z. R. In *Developments in Block Copolymers—I*; Goodman, I., Ed.; Applied Science: London, 1982.
(6) Bravoskii, S. A. *Sov. Phys. JETP* **1975**, *41*, 85.
(7) (a) Bates, F. S.; Rosedale, J. H.; Fredrickson, G. H.; Glinka, C. J. *Phys. Rev. Lett.* **1988**, *61*, 2229. (b) Bates, F. S.; Rosedale, J. H.; Fredrickson, G. H. *J. Chem. Phys.* **1990**, *92*, 6255.
(8) Bates, F. S.; Wiltzius, P. *J. Chem. Phys.* **1989**, *91*, 3258.
(9) Berg, N. F. *Phys. Rev. Lett.* **1987**, *58*, 2718.
(10) Anastasiadis, S. H.; Fytas, G.; Vogt, S.; Gerharz, B.; Fischer, E. W. *Europhys. Lett.*, in press.
(11) (a) Quan, X.; Johnson, G. E.; Anderson, E. W.; Bates, F. S. *Macromolecules* **1989**, *22*, 2451. (b) Fytas, G.; Alig, I.; Rizos, A.; Kanetakis, J.; Kremer, F.; Roovers, J. C. *Polym. Prepr. (Am. Chem. Soc., Div. Polym. Chem.)* **1992**, *33*, 86. (c) Alig, I.; Kremer, F.; Fytas, G.; Roovers, J. C. *Macromolecules* **1992**, *25*, 5277. (d) Rizos, A.; Fytas, G.; Roovers, J. C. *J. Chem. Phys.* **1992**, *97*, 6925.
(12) Shull, K. R.; Kramer, E. J.; Bates, F. S.; Rosedale, J. H. *Macromolecules* **1991**, *24*, 1383.
(13) Ehlich, D.; Takenaka, M.; Okamoto, S.; Hashimoto, T. *Macromolecules* **1993**, *26*, 189.
(14) Anastasiadis, S. H.; Russell, T. P.; Satija, S. K.; Majkrzak, C. F. *J. Chem. Phys.* **1990**, *92*, 5677.
(15) Burger, C.; Ruland, W.; Semenov, A. N. *Macromolecules* **1990**, *23*, 3339.
(16) Rosedale, J. H.; Bates, F. S. *Macromolecules* **1990**, *23*, 2329.
(17) Larson, R. G.; Fredrickson, G. H. *J. Chem. Phys.* **1987**, *86*, 1553.
(18) Fredrickson, G. H.; Helfand, E. *J. Chem. Phys.* **1988**, *89*, 5890.
(19) Kawasaki, K.; Sekimoto, K. *Macromolecules* **1989**, *22*, 3063.
(20) Doi, M.; Edwards, S. F. *The Theory of Polymer Dynamics*; Oxford University Press: Oxford, U.K., 1986.
(21) Parkhurst, H. J.; Jonas, J. *J. Chem. Phys.* **1975**, *63*, 2705.
(22) Gerharz, B.; Wagner, Th.; Ballauff, M.; Fischer, E. W. *Polym. Commun.* **1992**, *33*, 3561.
(23) Stühn, B. *J. Polym. Sci., Polym. Phys. Ed.* **1992**, *30*, 1013.
(24) Gerharz, B.; Meier, G.; Fischer, E. W. *J. Chem. Phys.* **1990**, *92*, 7110.
(25) Gerharz, B.; Vogt, S.; Fischer, E. W.; Fytas, G. *J. Prog. Colloid Polym. Sci.* **1993**, *91*, 58.
(26) Gerharz, B. Ph.D. Thesis, University of Mainz, 1991.
(27) Antonietti, M.; Coutardin, J.; Sillescu, H. *Macromolecules* **1986**, *19*, 793.
(28) Williams, M. L.; Landel, R. F.; Ferry, J. D. *J. Am. Chem. Soc.* **1955**, *77*, 3701.
(29) Momper, B. Ph.D. Thesis, University of Mainz, 1990.
(30) (a) Balsara, N. P.; Stepanek, P.; Lodge, T. P.; Tirrell, M. *Macromolecules* **1991**, *24*, 6227. (b) Balsara, N. P.; Eastman, C. E.; Foster, M. D.; Lodge, T. P.; Tirrell, M. *Makromol. Chem., Macromol. Symp.* **1991**, *45*, 213.
(31) Ferry, J. D. *Viscoelastic Properties of Polymers*, 3rd ed.; Wiley: New York, 1980. Pakula, T. Private communication.
(32) (a) Akcasu, A. Z.; Benmouna, M.; Benoit, H. *Polymer* **1986**, *27*, 1935. (b) Akcasu, A. Z.; Tombakoglu, M. *Macromolecules* **1990**, *23*, 607.
(33) Borsali, R.; Vilgis, T. A. *J. Chem. Phys.* **1990**, *93*, 3610.
(34) (a) Borsali, R.; Fischer, E. W.; Benmouna, M. *Phys. Rev. A* **1991**, *43*, 5732. (b) Borsali, R.; Benoit, H.; Legrand, J.-F.; Duval, M.; Picot, C.; Benmouna, M.; Farago, B. *Macromolecules* **1989**, *22*, 4119.
(35) Anastasiadis, S. H.; Fytas, G.; Vogt, S.; Fischer, E. W. *Phys. Rev. Lett.* **1993**, *70*, 2415.
(36) Vogt, S.; Gerharz, B.; Fischer, E. W.; Fytas, G. *Macromolecules* **1992**, *25*, 5986.
(37) Du'Chesne, A. Ph.D. Thesis, University of Mainz, 1991.
(38) Inoue, T.; Kishine, M.; Nemoto, N.; Kurata, M. *Macromolecules* **1989**, *22*, 495.
(39) Jian, T.; Anastasiadis, S. H.; Fytas, G.; Kotaka, T.; Adachi, K. *Macromolecules*, submitted for publication.